Incorporation of Terminal Constraints in the FDTD Analysis of Transmission Lines

Clayton R. Paul, *Fellow, IEEE*

Abstract— **A method of incorporating lumped terminal conditions into a finite-difference, time-domain (FDTD) analysis of multiconductor transmission lines is given. The method provides an exact solution of the transmission-line equations via the FDTD technique when the line discretization, Δz, and the time discretization, Δt, are chosen such that $\Delta t = \Delta z/v$ where v is the phase velocity of propagation on the line. Examples are given to show that in the case of a multiconductor line in an inhomogeneous medium where the mode velocities are not identical, the method gives accurate results with a minimum of computational effort.**

I. Introduction

THE transverse electromagnetic or TEM-mode model of an $(n+1)$-conductor, uniform multiconductor transmission line (MTL) is embodied in the MTL equations as [1]

$$\frac{\partial}{\partial z}\boldsymbol{V}(z,t) + \boldsymbol{R}\boldsymbol{I}(z,t) + \boldsymbol{L}\frac{\partial}{\partial t}\boldsymbol{I}(z,t) = \boldsymbol{0} \tag{1a}$$

$$\frac{\partial}{\partial z}\boldsymbol{I}(z,t) + \boldsymbol{G}\boldsymbol{V}(z,t) + \boldsymbol{C}\frac{\partial}{\partial t}\boldsymbol{V}(z,t) = \boldsymbol{0} \tag{1b}$$

where $\boldsymbol{V}$ and $\boldsymbol{I}$ are $n \times 1$ vectors of the line voltages (with respect to the reference conductor) and line currents, respectively. The line cross-sectional dimensions are contained in the $n \times n$ per-unit-length parameter matrices of $\boldsymbol{R}$ (resistance), $\boldsymbol{L}$ (inductance), $\boldsymbol{G}$ (conductance), and $\boldsymbol{C}$ (capacitance). The position along the line is denoted as z and time is denoted as t. The frequency-domain analysis of uniform multiconductor transmission lines is a straightforward computational task whether the line is considered lossless or lossy [1]. The time-domain analysis of MTL's is also simple if the line is considered lossless [1]. The time-domain analysis of *lossy* MTL's is considerably more difficult for several reasons. A primary reason is that the resistive losses of the conductors are due to skin effect and vary with frequency as $\sqrt{f}$. The representation of this frequency dependence in the time domain is a convolution which presents computational problems in a direct, time-domain solution of the MTL equations [2]. These problems have led to the use of other solution methods for the time-domain analysis of *lossy* MTL's. One of the important approximate solution techniques is the Finite-Difference, Time-Domain method or FDTD [3]–[6]. In that method, the line axis z is discretized in Δz increments or *spatial cells*, the time variable t is discretized in Δt increments or *temporal cells*, and the derivatives in the MTL equations are approximated by finite differences. The solution voltages and currents are obtained at these discrete points and represent an approximate solution of the MTL equations. In general, the accuracy of the solution depends on having sufficiently small spatial and temporal cell sizes. The FDTD method has been used successfully to solve more general electromagnetics problems wherein lossy, nonlinear, and/or inhomogeneous media may be considered. The spatial and temporal independent variables of the time-domain Maxwell's equations are similarly discretized, and the boundary conditions are readily incorporated [7].

MTL's are simply one-dimensional versions of wave propagation embodied in the three-dimensional Maxwell's equations for the special case of the TEM or quasi-TEM mode of propagation. An important difference is the boundary conditions. For the full-wave electromagnetics problem, zero tangential electric field on the surface of perfect conductors is a primary boundary condition. Scattering problems can be handled with the absorbing boundary condition [7]. In the case of MTL's, the boundary conditions are lumped loads at the two ends of the line, $z = 0$ and $z = \mathcal{L}$ for a line of length $\mathcal{L}$. Linear, resistive such terminations can be characterized by Generalized Thevenin Equivalents as [1]

$$\boldsymbol{V}(0,t) = \boldsymbol{V}_S - \boldsymbol{R}_S\boldsymbol{I}(0,t) \tag{2a}$$

$$\boldsymbol{V}(\mathcal{L},t) = \boldsymbol{V}_L + \boldsymbol{R}_L\boldsymbol{I}(\mathcal{L},t) \tag{2b}$$

or a similar Generalized Norton Equivalent or a combination of the two. The essential question addressed in this paper is how we shall incorporate these lumped terminal constraints into the FDTD solution of the MTL equations. In order to insure stability in the FDTD solution, the discrete voltage and current solution points are not physically located at the same point but are staggered one-half cell apart [7]. However, the lumped terminal constraints such as in (2) require that the current and voltages solution points be collocated. One approximate approach to addressing this dilemma has been to interpolate the current solution points to the nearest adjacent voltage solution point and then use (2) [3]. It also turns out that the discrete voltages and currents must be similarly staggered or "interlaced" in time with the time points for the voltages and for the currents being spaced one-half temporal cell apart [7]. The method shown in this paper provides an exact incorporation of the lumped terminal conditions in (2). Although the exactness of this incorporation will only be proven for lossless lines, it is expected that it carries over to a similar degree to the case of lossy lines.

Manuscript received May 24, 1993; revised October 28, 1993.

The author is with the Department of Electrical Engineering, University of Kentucky, Lexington, KY 40506.

IEEE Log Number 9216516.

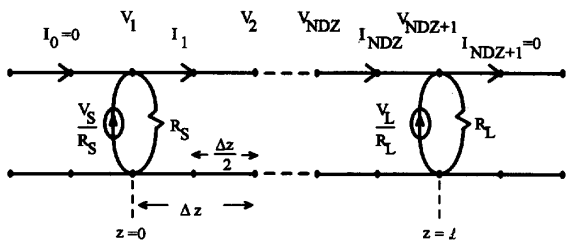

Fig. 1. The spatial discretization of the line showing location of the interlaced voltage and current solution points.

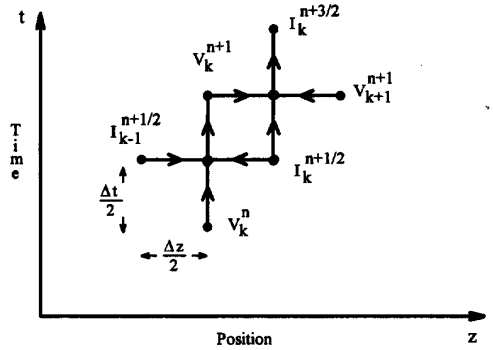

Fig. 2. The relation between the spatial and temporal discretizations to achieve second-order accuracy in the discretization of the derivatives.

II. The FDTD Formulation

In order to illustrate the method, consider a two-conductor uniform line. To incorporate the terminal conditions and provide some generality assume that the line is lossy and has an incident electromagnetic field as its excitation in addition to the lumped sources in (2). The transmission-line equations become [3]

$$\frac{\partial V(z,t)}{\partial z} + l\frac{\partial I(z,t)}{\partial t} + rI(z,t) = V_F(z,t) \tag{3a}$$

$$\frac{\partial I(z,t)}{\partial z} + c\frac{\partial V(z,t)}{\partial t} + gV(z,t) = I_F(z,t) \tag{3b}$$

where the incident field gives rise to distributed voltage and current sources V_F and I_F. The FDTD technique seeks to approximate the derivatives in these equations with regard to the discrete solution points defined by the spatial and temporal cells. It was pointed out in [9] that there are many ways of approximating these derivatives yet only certain ones give the exact solution. Maxwell's equations (Faraday's and Ampere's laws) are *coupled, first-order* partial differential equations like the MTL equations. Applications of the FDTD method to the full-wave solution of Maxwell's equations have shown that accuracy and stability of the solution is achieved if we choose the electric and magnetic field solution points to alternate in space and be separated by one-half the position discretization, e.g., $\Delta z/2$, and we choose the solution times for these two quantities to also be interlaced in time and separated by $\Delta t/2$ [7]. To incorporate this experience into the FDTD solution of the transmission-line equations, we divide the line into NDZ sections each of length Δz as shown in Fig. 1. Similarly, we divide the total solution time into segments of length Δt. In order to insure stability of the discretization and to insure second-order accuracy we interlace the NDZ + 1 voltage points, $V_1, V_2, \cdots, V_{\mathrm{NDZ}}, V_{\mathrm{NDZ}+1}$, and the NDZ current points, $I_1, I_2, \cdots, I_{\mathrm{NDZ}}$, as shown in Fig. 2. Each voltage and adjacent current solution point is separated by $\Delta z/2$. In addition, the time points are also interlaced, and each voltage time point and adjacent current time point are separated by $\Delta t/2$ as illustrated in Fig. 2. The finite difference approximations to (3) become [3]

$$\frac{V_{k+1}^{n+1} - V_k^{n+1}}{\Delta z} + l\frac{I_k^{n+3/2} - I_k^{n+1/2}}{\Delta t} + r\frac{I_k^{n+3/2} + I_k^{n+1/2}}{2} = \frac{V_F^{n+3/2} + V_F^{n+1/2}}{2} \tag{4a}$$

$$\frac{I_k^{n+1/2} - I_{k-1}^{n+1/2}}{\Delta z} + c\frac{V_k^{n+1} - V_k^n}{\Delta t} + g\frac{V_k^{n+1} + V_k^n}{2} = \frac{I_F^{n+1} + I_F^n}{2} \tag{4b}$$

where we denote

$$V_i^j \equiv V((i-1)\Delta z, j\Delta t) \tag{5a}$$

$$I_i^j \equiv I\left((i-\frac{1}{2})\Delta z, j\Delta t\right) \tag{5b}$$

and n and k are integers. Solving these gives the required recursion relations:

$$\left(l\frac{\Delta z}{\Delta t} + \frac{r}{2}\Delta z\right)I_k^{n+3/2} = \left(l\frac{\Delta z}{\Delta t} - \frac{r}{2}\Delta z\right)I_k^{n+1/2} - \left(V_{k+1}^{n+1} - V_k^{n+1}\right) + \frac{\Delta z}{2}\left(V_F^{n+3/2} + V_F^{n+1/2}\right) \tag{6a}$$

$$\left(c\frac{\Delta z}{\Delta t} + \frac{g}{2}\Delta z\right)V_k^{n+1} = \left(c\frac{\Delta z}{\Delta t} - \frac{g}{2}\Delta z\right)V_k^n - \left(I_k^{n+1/2} - I_{k-1}^{n+1/2}\right) + \frac{\Delta z}{2}\left(I_F^{n+1} + I_F^n\right). \tag{6b}$$

These are solved in a "bootstrapping" fashion. First the voltages along the line are solved for a fixed time from (6b) in terms of the previous solutions and then the currents are solved for from (6a) in terms of these and previous values. The solution starts with an initially relaxed line having zero voltage and current values.

Next consider incorporating the terminal conditions. Referring to Fig. 1, we represent these as Norton equivalents where we allow for lumped sources and loads at $z = 0$ characterized by $I_S = V_S/R_S$ and R_S and at $z = \mathcal{L}$ characterized by $I_L = V_L/R_L$ and R_L. Substitute into (6b) for $k = 1$

$$I_0 = 0 \tag{7a}$$

$$g = \frac{1}{R_S\Delta z} \tag{7b}$$

$$I_F = \frac{V_S}{R_S\Delta z}. \tag{7c}$$

Similarly, we impose the terminal constraints at $z = \mathcal{L}$ by substituting into (6b) for $k = \text{NDZ} + 1$:

$$I_{\text{NDZ}+1} = 0 \tag{8a}$$

$$g = \frac{1}{R_L \Delta z} \tag{8b}$$

$$I_F = \frac{V_L}{R_L \Delta z}. \tag{8c}$$

We will also show that setting $I_0 = I_{\text{NDZ}+1} = 0$ for $k = 1$ and $k = \text{NDZ} + 1$ in (6b) requires that we replace $c\Delta z$ with $c\Delta z/2$ in *only those two equations*. Equation (6b) for all other $k, k = 2, 3, \cdots$, NDZ, must use $c\Delta z$. In this section we will consider lossless lines so we set

$$r = V_F = 0 \tag{9a}$$

in (6a) for all k and set

$$g = I_F = 0 \tag{9b}$$

in (6b) for $k = 2, 3, \cdots$, NDZ. This gives the final difference equations to be solved. Equation (6b) for $k = 1$

$$\begin{aligned} V_1^{n+1} &= \left[R_S \frac{c}{2}\frac{\Delta z}{\Delta t} + \frac{1}{2}\right]^{-1} \left\{ \left[R_S \frac{c}{2}\frac{\Delta z}{\Delta t} - \frac{1}{2}\right] V_1^n \right. \\ &\quad \left. - R_S \left(I_1^{n+1/2} - \underbrace{I_0^{n+1/2}}_{=0} \right) + \frac{(V_S^{n+1} + V_S^n)}{2} \right\} \\ &= \left[R_S \frac{c}{2}\frac{\Delta z}{\Delta t} + \frac{1}{2}\right]^{-1} \left\{ \left[R_S \frac{c}{2}\frac{\Delta z}{\Delta t} - \frac{1}{2}\right] V_1^n \right. \\ &\quad \left. - R_S (I_1^{n+1/2}) + \frac{(V_S^{n+1} + V_S^n)}{2} \right\}. \end{aligned} \tag{10a}$$

Equation (6b) for $k = 2, 3, \cdots$, NDZ

$$V_k^{n+1} = V_k^n - \frac{\Delta t}{\Delta z} c^{-1} \left(I_k^{n+1/2} - I_{k-1}^{n+1/2} \right). \tag{10b}$$

Equation (6b) for $k = \text{NDZ} + 1$

$$\begin{aligned} V_{\text{NDZ}+1}^{n+1} &= \left[R_L \frac{c}{2}\frac{\Delta z}{\Delta t} + \frac{1}{2}\right]^{-1} \left\{ \left[R_L \frac{c}{2}\frac{\Delta z}{\Delta t} - \frac{1}{2}\right] V_{\text{NDZ}+1}^n \right. \\ &\quad \left. - R_L \left(\underbrace{I_{\text{NDZ}+1}^{n+1/2}}_{=0} - I_{\text{NDZ}}^{n+1/2} \right) + \frac{(V_L^{n+1} + V_L^n)}{2} \right\} \\ &= \left[R_L \frac{c}{2}\frac{\Delta z}{\Delta t} + \frac{1}{2}\right]^{-1} \left\{ \left[R_L \frac{c}{2}\frac{\Delta z}{\Delta t} - \frac{1}{2}\right] V_{\text{NDZ}+1}^n \right. \\ &\quad \left. + R_L \left(I_{\text{NDZ}}^{n+1/2} \right) + \frac{(V_L^{n+1} + V_L^n)}{2} \right\}. \end{aligned} \tag{10c}$$

Equation (6a) for $k = 1, 2, \cdots$, NDZ

$$I_k^{n+3/2} = I_k^{n+1/2} - \frac{\Delta t}{\Delta z} l^{-1} (V_{k+1}^{n+1} - V_k^{n+1}). \tag{10d}$$

The voltages and currents are solved by iterating k for a fixed time and then iterating time. The initial conditions of zero voltage and current are used to start the iteration. The condition for this set of recursion relations to be stable is the Courant condition [7]

$$\Delta t \leq \frac{\Delta z}{v} \tag{11}$$

which amounts to the condition that the time step must be no greater than the propagation time over each cell. The Δz discretization is chosen sufficiently small such that each Δz section is *electrically small* at the significant spectral components of the source voltages, $V_S(t)$ and $V_L(t)$.

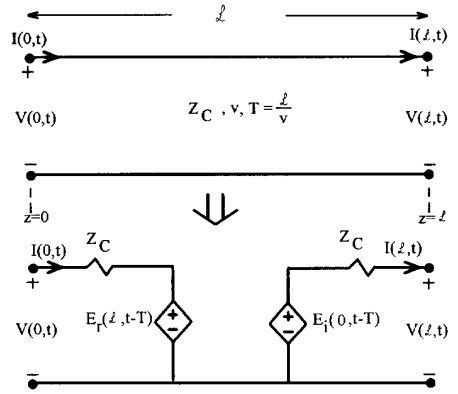

Fig. 3. Illustration of an exact model of the transmission line in terms of time-delayed controlled sources.

III. The Exact Solution

It is not obvious that the method of incorporating the terminal constraints by using the distributed conductance g and distributed induced field source I_F in (4b) or (6b) and making the correspondences as in (7) and (8) provide an *exact solution* of the transmission-line equations via the FDTD method when the time and position steps are chosen exactly for the Courant condition (referred to as the "magic time step" [7]). Nor is it obvious that we must use $c\Delta z/2$ in the end sections and $c\Delta z$ in the interior sections in (6b) in order to provide this exact solution. We now set out to prove this.

In order to show this we will utilize an exact solution for a lossless line that is referred to as the method of characteristics or Branin's method [1], [10]. The method of characteristics provides an exact solution of the transmission line equations via the model of Fig. 3. This is the model implemented in the SPICE circuit analysis program which can be extended to the exact characterization of lossless MTL's [1]. The equations resulting from this model are

$$V(0,t) = Z_C I(0,t) + E_r(\mathcal{L}, t - T) \tag{12a}$$

where

$$E_r(\mathcal{L}, t - T) = V(\mathcal{L}, t - T) - Z_C I(\mathcal{L}, t - T) \tag{12b}$$

and

$$V(\mathcal{L}, t) = -Z_C I(\mathcal{L}, t) + E_i(0, t - T) \tag{13a}$$

where

$$E_i(0, t - T) = V(0, t - T) + Z_C I(0, t - T) \tag{13b}$$

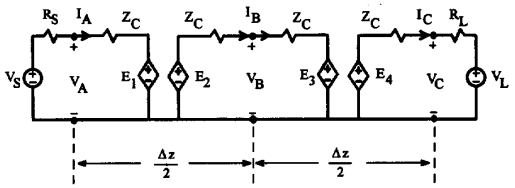

Fig. 4. Representation of the discretized line in terms of the exact model of Fig. 3.

where the characteristic impedance is denoted as

$$Z_C = \sqrt{\frac{l}{c}} = vl = \frac{1}{vc}. \tag{14}$$

The time-delayed controlled sources, E_r, and E_i, represent the effects of the voltages and currents at the opposite ends of the line which are delayed in time by the one-way transit time of the line

$$T = \frac{\mathcal{L}}{v}. \tag{15}$$

This is an *exact* representation of a lossless, two-conductor line. Without loss of generality, let us divide the line into one section of length Δz and choose solution voltages V_A and V_C at the ends and a solution current, I_B, at the midpoint as shown in Fig. 4. The remaining voltage and currents, I_A, V_B, I_C, would not be solved for in a FDTD solution and are auxiliary variables here. Each half of length $\Delta z/2$ is modeled with its own exact solution with reference to Fig. 3 with time delay $\tau/2$ where

$$\tau = \frac{\Delta z}{v}. \tag{16}$$

In order to simplify the derivation, we use the *difference operator*:

$$D^{\pm m} f(t) = f(t \pm m\tau). \tag{17}$$

The resulting equations relating all voltages and currents in Fig. 4 are

$$V_A = Z_C I_A + D^{-1/2}(V_B - Z_C I_B) \tag{18a}$$
$$V_B = -Z_C I_B + D^{-1/2}(V_A + Z_C I_A) \tag{18b}$$
$$V_B = Z_C I_B + D^{-1/2}(V_C - Z_C I_C) \tag{18c}$$
$$V_C = -Z_C I_C + D^{-1/2}(V_B + Z_C I_B). \tag{18d}$$

We will now derive the recursion relations in (10) from this exact model thereby proving the previous method of incorporating the terminal constraints into the FDTD solution is exact when the temporal and spatial cell sizes are chosen as the "magic time step" such that

$$\Delta t = \frac{\Delta z}{v}. \tag{19}$$

First we will derive (10a). For these purposes, we let $V_A = V_1, I_B = I_1$, and $V_C = V_2$. The objective is to eliminate I_A, V_B, I_C from these equations and write the result in terms of V_1, I_1, and V_2. The terminal conditions at $z = 0$ are

$$I_A = \frac{V_S}{R_S} - \frac{V_1}{R_S}. \tag{20}$$

Substituting (20) into (18a) and (18b) gives

$$V_1 = \frac{Z_C}{R_S} V_S - \frac{Z_C}{R_S} V_1 + D^{-1/2}(V_B - Z_C I_1) \tag{21a}$$
$$V_B = -Z_C I_1 + D^{-1/2}\left(V_1 + \frac{Z_C}{R_S} V_S - \frac{Z_C}{R_S} V_1\right). \tag{21b}$$

Operating on (21a) with D and (21b) with $D^{1/2}$ and substituting gives

$$\left(1 + \frac{Z_C}{R_S}\right) DV_1 = \left(1 - \frac{Z_C}{R_S}\right) V_1 - 2Z_C D^{1/2} I_1 + \frac{Z_C}{R_S}(DV_S + V_S). \tag{22}$$

Rewriting (multiplying both sides by $R_S/2Z_C$) gives

$$DV_1 = \left(\frac{1}{2}\frac{R_S}{Z_C} + \frac{1}{2}\right)^{-1} \left\{ \left(\frac{1}{2}\frac{R_S}{Z_C} - \frac{1}{2}\right) V_1 - R_S D^{1/2} I_1 + \frac{1}{2}(DV_S + V_S) \right\}. \tag{23}$$

In order to show that (23) is equivalent to (10a) for the magic time step in (19) we substitute (19) along with the relationship between the per-unit-length capacitance and characteristic impedance, $vc = Z_C^{-1}$, into (10a) which gives (23). This shows that (10a) is the proper FDTD relation for the end section and that for the end section we must use $c\Delta z/2$ rather that $c\Delta z$.

Similarly, we may obtain (10c) for the last Δz section at $z = \mathcal{L}$ by letting $V_A = V_{\mathrm{NDZ}}$, $I_B = I_{\mathrm{NDZ}}$, and $V_C = V_{\mathrm{NDZ+1}}$. The equations are

$$V_{\mathrm{NDZ}} = Z_C I_A + D^{-1/2}(V_B - Z_C I_{\mathrm{NDZ}}) \tag{24a}$$
$$V_B = -Z_C I_{\mathrm{NDZ}} + D^{-1/2}(V_{\mathrm{NDZ}} + Z_C I_A) \tag{24b}$$
$$V_B = Z_C I_{\mathrm{NDZ}} + D^{-1/2}(V_{\mathrm{NDZ+1}} - Z_C I_C) \tag{24c}$$
$$V_{\mathrm{NDZ+1}} = -Z_C I_C + D^{-1/2}(V_B + Z_C I_{\mathrm{NDZ}}). \tag{24d}$$

The objective is to incorporate the lumped terminal conditions at $z = \mathcal{L}$ and to eliminate I_A, V_B, I_C to give an equations in V_{NDZ}, I_{NDZ}, $V_{\mathrm{NDZ+1}}$ which, for the magic time step of (19), is equivalent to (10c). Again this can be readily done as above.

The remaining tasks are to show that (10b) and (10d) for the interior solution nodes are correct for the magic time step. First we show that (10b) is correct by letting $I_A = I_{k-1}$, $V_B = V_k$, and $I_C = I_k$ in (18) and eliminating V_A, I_B, and V_C. Equations (18) become

$$V_A = Z_C I_{k-1} + D^{-1/2}(V_k - Z_C I_B) \tag{25a}$$
$$V_k = -Z_C I_B + D^{-1/2}(V_A + Z_C I_{k-1}) \tag{25b}$$
$$V_k = Z_C I_B + D^{-1/2}(V_C - Z_C I_k) \tag{25c}$$
$$V_C = -Z_C I_k + D^{-1/2}(V_k + Z_C I_B). \tag{25d}$$

Operating on (25a) with $D^{1/2}$ and (25b) with D and substituting gives

$$DV_k = V_k + 2Z_C D^{1/2} I_{k-1} - Z_C(DI_B + I_B). \tag{26}$$

Similarly, operating on (25d) with $D^{-1/2}$ and substituting into (25c) gives

$$DV_k = V_k - 2Z_C D^{1/2} I_k + Z_C(DI_B + I_B). \tag{27}$$

Adding (26) and (27) gives

$$DV_k = V_k + Z_C D^{1/2}(I_k - I_{k-1}). \tag{28}$$

Substituting the magic time step given in (19) along with $vc = Z_C^{-1}$ into (10b) we obtain (28) demonstrating their equivalence. Similarly, we can demonstrate the correctness of (10d) from the circuit model of Fig. 4 by letting $V_A = V_k$, $I_B = I_k$, and $V_C = V_{k+1}$ in (18) and eliminating I_A, V_B, and I_C. Equations (18) become

$$V_k = Z_C I_A + D^{-1/2}(V_B - Z_C I_k) \tag{29a}$$

$$V_B = -Z_C I_k + D^{-1/2}(V_k + Z_C I_A) \tag{29b}$$

$$V_B = Z_C I_k + D^{-1/2}(V_{k+1} - Z_C I_C) \tag{29c}$$

$$V_{k+1} = -Z_C I_C + D^{-1/2}(V_B + Z_C I_k). \tag{29d}$$

The objective is to eliminate I_A, V_B, I_C from these equations and to show that they are equivalent to (10d) for the magic time step of (19). Subtracting (29a) from (29d) and operating on the result with D gives

$$D(V_{k+1} - V_k) = -Z_C D I_C - Z_C D I_A + 2Z_C D^{1/2} I_k. \tag{30}$$

Operating on (29b) and (29c) with $D^{3/2}$ and subtracting gives

$$0 = D(V_{k+1} - V_k) - Z_C D I_C - Z_C D I_A + 2Z_C D^{3/2} I_k. \tag{31}$$

Substituting (31) into (30) gives

$$D^{3/2} I_k - D^{1/2} I_k = -Z_C^{-1} D(V_{k+1} - V_k). \tag{32}$$

Substituting the magic time step of (19) along with $Z_C = vl$ into (10d) we obtain (32) demonstrating their equivalence.

IV. Extensions and Observations

The above demonstrated that the finite-difference recursion relations in (10) are an exact representation of a two-conductor, lossless line for the magic time step of (19). In this section we will extend those to MTL's and also provide an intuitive derivation.

A common way of approximating transmission lines is with lumped-circuit iterative approximations [1]. One such representation is the Lumped Pi representation wherein the line is divided into Δz segments and the per-unit-length distributed parameters of inductance and capacitance are represented by lumped elements. Fig. 5 shows a Lumped Pi model of the line with the division points chosen at the above finite-difference solution voltage nodes, $V_1, V_2, \cdots, V_{\mathrm{NDZ}}, V_{\mathrm{NDZ+1}}$. Each Δz segment is represented by its inductance,$l\Delta z$, and the capacitance is split and placed at the ends of each section as $(c/2)\Delta z$. The finite-difference current solution points $I_1, I_2, \cdots, I_{\mathrm{NDZ}}$ are through the inductors at the center of each section. Observing the interlacing of the solution time points

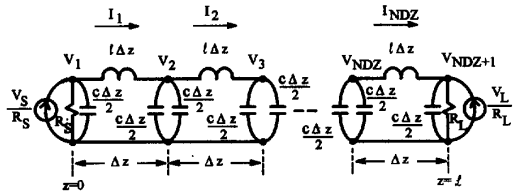

Fig. 5. Equivalent representation of the FDTD discretization using the Lumped Pi circuit model.

as in Fig. 2, one can derive (10) directly from this circuit. In doing so, it is important to observe the relations in Fig. 2. This shows that, although (10) were derived for resistive terminations, they can be extended to dynamic terminations so long as the derivatives in those relations are approximated according to Fig. 2. Similarly, line losses and incident field effects can be incorporated using (6). It was shown in [11] that the circuit of Fig. 5 is equivalent to a method of moments (MOM) Galerkin solution for the frequency-domain and pulse-expansion functions. This implies a strong connection between the FDTD solution method and the MOM method as well as the Transmission Line Matrix (TLM) method [12]. Additionally, although the termination constraints were modeled as shunt elements it appears that a dual procedure could be developed for modeling them as series elements. In this case, the Lumped T equivalent would replace the circuit of Fig. 5 [1].

The recursion relations in (10) were derived for two-conductor lines. These can be similarly derived in like fashion for a multiconductor line whose terminations are described by (2) resulting in

$$\boldsymbol{V}_1^{n+1} = \left[\frac{\Delta z}{\Delta t}\boldsymbol{R}_S\boldsymbol{C} + \mathbf{1}\right]^{-1}\left\{\left[\frac{\Delta z}{\Delta t}\boldsymbol{R}_S\boldsymbol{C} - \mathbf{1}\right]\boldsymbol{V}_1^n - 2\boldsymbol{R}_S\boldsymbol{I}_1^{n+1/2} + \left(\boldsymbol{V}_S^{n+1} + \boldsymbol{V}_S^n\right)\right\} \tag{33a}$$

$$\boldsymbol{V}_k^{n+1} = \boldsymbol{V}_k^n - \frac{\Delta t}{\Delta z}\boldsymbol{C}^{-1}\left(\boldsymbol{I}_k^{n+1/2} + \boldsymbol{I}_{k-1}^{n+1/2}\right) \qquad k = 2, \cdots, \mathrm{NDZ} \tag{33b}$$

$$\boldsymbol{V}_{\mathrm{NDZ+1}}^{n+1} = \left[\frac{\Delta z}{\Delta t}\boldsymbol{R}_L\boldsymbol{C} + \mathbf{1}\right]^{-1}\left\{\left[\frac{\Delta z}{\Delta t}\boldsymbol{R}_L\boldsymbol{C} - \mathbf{1}\right]\boldsymbol{V}_{\mathrm{NDZ+1}}^n + 2\boldsymbol{R}_L\boldsymbol{I}_{\mathrm{NDZ+1}}^{n+1/2} + \left(\boldsymbol{V}_L^{n+1} + \boldsymbol{V}_L^n\right)\right\} \tag{33c}$$

$$\boldsymbol{I}_k^{n+3/2} = \boldsymbol{I}_k^{n+1/2} - \frac{\Delta t}{\Delta z}\boldsymbol{L}^{-1}\left(\boldsymbol{V}_{k+1}^{n+1} + \boldsymbol{V}_k^{n+1}\right) \qquad k = 1, \cdots, \mathrm{NDZ}. \tag{33d}$$

Dynamic loads can be incorporated as above by deriving this result from the multiconductor version of the equivalent circuit in Fig. 5.

V. Computed Results

We will apply these results to two transmission line problems. The first is a lossless, two-conductor line having $V_S(t) =$

30 V, $R_S = 0\ \Omega$, $V_L(t) = 0$, and $R_L = 100\ \Omega$. The line is of length $\mathcal{L} = 400$ m and has $v = 2 \times 10^8$ m/s and $Z_C = 50\ \Omega$. The exact solution was obtained in [1] by hand and with the SPICE program. In all computed results we will designate

$$\Delta z = \frac{\mathcal{L}}{\text{NDZ}} \tag{34a}$$

$$\Delta t = \frac{\text{Final Solution Time}}{\text{NDT}}. \tag{34b}$$

The Courant condition for stability of the FDTD solution given in (11) translates to

$$\text{NDT} \geq \text{NDZ}\,\frac{v \times \text{Final Solution Time}}{\mathcal{L}}. \tag{35}$$

The magic time step in (19) occurs for an equality in this expression. Fig. 6 shows the results for various discretizations. Recall that the Δz discretization is chosen such that each section is *electrically small* for the significant spectral components of the source waveform. Then the Δt discretization is chosen to satisfy the Courant condition or the magic time step. It is shown in [1] that for a pulse having a rise time of τ_r, the high-frequency components of the spectrum roll off at -40 dB/decade above a frequency of $1/\pi\tau_r$. In this problem, the pulse has $\tau_r = 0$ so we would not expect adequate characterization of all spectral components for *other than the magic time step*. Fig. 6 shows the results using only one spatial discretization of the line, NDZ = 1, and the magic time step of NDT = 10. Those solution points denoted as $\times$'s yield the exact solution supporting the above results. If we further subdivide the line into NDZ = 200 and use the magic time step of NDT = 2000 we again obtain the *exact solution*. And finally, Fig. 6 shows the results for NDZ = 200 but the time step is not equal to the magic time step but satisfies the Courant condition. Observe that there is considerable "ringing" or Gibbs-like phenomena on the leading edges of the waveform. Therefore, if we do not choose to use the magic time step we must further reduce the Δz discretization (increase NDZ) in order to reduce this ringing since the high-frequency spectral content extends to very high frequencies for this case of $\tau_r = 0$. Here the high-frequency spectral content rolls off only as -20 dB/decade [1]. This illustrates an interesting "quirk" in the FDTD solution: the magic time step gives the exact result but for the same Δz discretization, reducing Δt slightly below the magic time step causes significant deviation from the true solution depending on the spectral content of the waveform. To illustrate this further, Fig. 7 shows these results for a nonzero rise time of $\tau_r = 0.1\ \mu$s. The high-frequency spectral content of this waveform rolls off at -40 dB/decade above $1/\pi\tau_r = 3.18$ MHz. For NDZ = 200, $\Delta z = 2$ m which is $\lambda/10$ at 15 MHz. So a discretization of NDZ = 200 should sufficiently process the significant spectral components of this waveform. Fig. 7 shows that the severe ringing encountered for the zero rise time source and Δt less than the magic time step (NDZ = 200, NDT = 4000) is reduced considerably as expected but is not eliminated.

The next problem is a three-conductor line consisting of three 15-mil-wide lands on a glass-epoxy printed-circuit board that are separated edge-to-edge by 45 mils [1]. The line length

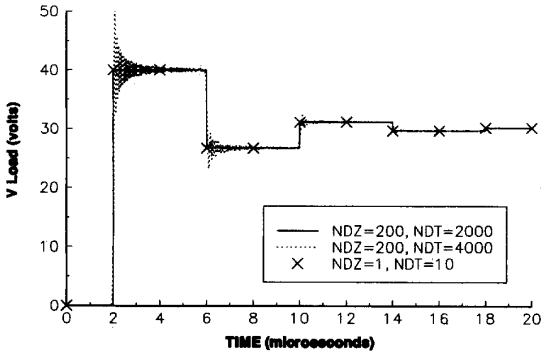

Fig. 6. Solution for a line of length 400 m and a 100-Ω load for $V_S(t)$as a 30-V pulse with a zero rise time, $\tau_r = 0$.

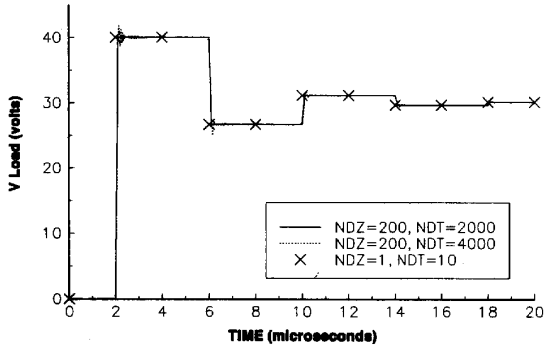

Fig. 7. Solution for the problem of Fig. 6 for a pulse having $\tau_r = 0.1\ \mu$s.

is 0.254 m and the per-unit-length parameters are

$$\boldsymbol{L} = \begin{bmatrix} 1.10418 & 0.690094 \\ 0.690094 & 1.38019 \end{bmatrix}\ \mu\text{H/m}$$

$$\boldsymbol{C} = \begin{bmatrix} 40.6280 & -20.3140 \\ -20.3140 & 29.7632 \end{bmatrix}\ \text{pF/m}.$$

The terminal conditions are

$$\boldsymbol{V}_S(t) = \begin{bmatrix} 0 \\ V_S(t) \end{bmatrix}$$

$$\boldsymbol{R}_S = \begin{bmatrix} 50 & 0 \\ 0 & 50 \end{bmatrix}\ \Omega$$

$$\boldsymbol{V}_L(t) = \begin{bmatrix} 0 \\ 0 \end{bmatrix}$$

$$\boldsymbol{R}_L = \begin{bmatrix} 50 & 0 \\ 0 & 50 \end{bmatrix}\ \Omega$$

where $V_S(t)$ is a 1-V pulse having a rise time of $\tau_r = 6.25$ ns. Fig. 8 shows the FDTD results compared to the *exact* results computed by Branin's method and implemented in SPICE [1]. The line has two mode velocities, $v_1 = 1.80065 \times 10^8$ m/s and $v_2 = 1.92236 \times 10^8$ m/s. The Δz discretization is chosen to make each section electrically short at $1/\pi\tau_r = 51$ MHz giving, using the smaller mode velocity v_1, $\Delta z < 0.353$ m. So we choose NDZ = 2. Using the larger mode velocity to set the magic time step gives NDT = 60. The comparison between the exact solution and the FDTD solution for the magic time step is excellent. Observe that even when the time discretization is

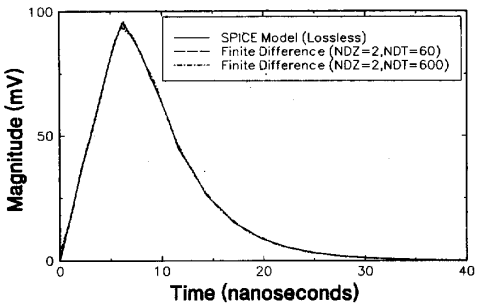

Fig. 8. Solution for the near-end crosstalk on a printed-circuit board having 50-Ω terminations and a 1-V pulse with a 6.25-ns rise time.

reduced from that of the magic time step, NDZ = 2, NDT = 600, the correlation remains excellent. This demonstrates that even in the case of MTL's in inhomogeneous media where the mode velocities are different so that the discretization can be chosen equal to the magic time step for only one of those velocities, the FDTD method can still give accurate results even though the other mode velocities do not satisfy the magic time step criterion.

VI. Summary and Conclusion

This paper has shown a method for incorporating lumped terminal constraints into an FDTD analysis of the transmission line equations. If the position and time discretizations are chosen to satisfy the magic time step, $\Delta t = \Delta z/v$, for a two-conductor line, the FDTD method yields the exact solution of the transmission-line equations within approximation or discretization error. In the case of MTL's in inhomogeneous media where the magic time step cannot be attained for both mode velocities, computed results demonstrated that excellent predictions can still be attained.

References

[1] C. R. Paul, *Introduction to Electromagnetic Compatibility*. New York: Wiley-Interscience, 1992.
[2] F. M. Tesche, "On the inclusion of losses in time-domain solutions of electromagnetic interaction problems," *IEEE Trans. Electromagn. Compat.*, vol. 32, no. 1, pp. 1–4, Feb. 1990.
[3] A. K. Agrawal, H. J. Price, and S. H. Gurbaxani, "Transient response of multiconductor transmission lines excited by a nonuniform electromagnetic field," *IEEE Trans. Electromagn. Compat.*, vol. EMC-22, no. 2, pp. 119–129, May 1980.
[4] D. F. Higgins, "Calculating transmission line transients on personal computers," in *Proc. IEEE Int. Symp. on Electromagnetic Compatibility* (Atlanta, GA, Aug. 25–27, 1987,).
[5] E. S. M. Mok and G. I. Costache, "Skin-effect considerations in transient response of a transmission line excited by an electromagnetic pulse," *IEEE Trans. Electromagn. Compat.*, vol. 34, no. 3, pp. 320–329, Aug. 1992.
[6] A. R. Djordjevic, T. S. Sarkar, and R. F. Harrington, "Time-domain response of multiconductor transmission lines," *Proc. IEEE*, vol. 75, no. 6, pp. 743–764, June 1987.
[7] K. Li, M. A. Tassoudi, R, T. Shin, and J. A. Kong, "Simulation of electromagnetic radiation and scattering using a finite difference-time domain technique," *Comput. Appl. in Eng. Education*, vol. 1, no, 1, pp. 45–62, Sept./Oct. 1992.
[8] C. R. Paul, "Literal solution for the time-domain crosstalk on lossless transmission lines," *IEEE Trans. Electromagn. Compat.*, vol. 34, no. 4, pp. 433–444, Nov. 1992.
[9] Z. Fazarinc, "Discretization of partial differential equations for computer evaluation," *Comput. Appl. in Eng. Education*, vol. 1, no. 1, pp. 73–85, Sept./Oct. 1992.
[10] F. H. Branin, Jr., "Transient analysis of lossless transmission lines," *Proc. IEEE*, vol. 55, pp. 2012–2013, 1967.
[11] R. F. Harrington, *Field Computation by Moment Methods*. New York: Macmillan, 1968.
[12] M. N. O. Sadiku, *Numerical Techniques in Electromagnetics*. Boca Raton, FL: CRC Press, 1992.

Clayton R. Paul (S'61–M'70–SM'79–F'87) was born in Macon, GA, on September 6, 1941. He received the B.S. degree from The Citadel, Charleston, SC, the M.S. degree from Georgia Institute of Technology, Atlanta, and the Ph.D. degree from Purdue University, Lafayette, IN, in 1963, 1964, and 1970, respectively, all in electrical engineering.

He has been a Member of the Faculty of the Department of Electrical Engineering at the University of Kentucky, Lexington, since 1971, and is currently Professor of Electrical Engineering. He is the author of seven textbooks on electrical engineering subjects and has published over 80 technical papers, the majority of which are in his primary research area of electromagnetic compatibility (EMC) of electronic systems. From 1970 to 1984, he conducted extensive research for the U.S. Air Force into modeling crosstalk in multiconductor transmission lines and printed circuits boards. From 1984 to 1990, he has served as a consultant to the IBM Corporation in the area of product EMC design.

Dr. Paul is a member of Tau Beta Pi and Eta Kappa Nu.